

Neutron Reflectivity Studies of Polymer Concentration Profiles at the Liquid/Air Interface

L. T. Lee,* O. Guiselin, B. Farnoux, and A. Lapp

Laboratoire Léon Brillouin (CEA-CNRS), CEN Saclay, 91191 Gif-sur-Yvette Cedex, France

Received August 20, 1990; Revised Manuscript Received November 9, 1990

ABSTRACT: The concentration profile of a linear flexible polymer adsorbed from good solvent at the liquid/air interface has been studied by neutron reflectivity. Two different isotopic compositions, deuterated polymer in protonated solvent and protonated polymer in deuterated solvent, have been considered; both systems furnish the same information concerning the physical properties of the adsorbed layer. The experimental results are interpreted in terms of predictions of scaling theory. In close proximity to the surface, there exists a monomer-rich zone, D , which is determined to be 10–15 Å thick and independent of polymer molecular weight and bulk concentration. Beyond D , the profile decreases with a self-similar structure with the monomer density scaling as $\phi(z) \sim z^{-4/3}$, where z is the distance from the surface. The reflectivity results are consistent with surface tension data and support a strong adsorption and weak coupling case for the system.

Introduction

When polymers are adsorbed at an interface, a concentration gradient develops. The profile of this gradient plays a central role in the field of colloidal stability. Measurements of the structural properties of the adsorbed layer, however, are not always simple and unambiguous for several reasons. First, due to its macromolecular dimension and flexibility, a polymer molecule can adopt numerous conformations both in the bulk solution and in the adsorbed state. Second, because of the number of adsorbable units, the polymer can attach itself at more than one point per molecule, resulting in a strong adsorption behavior even though the energy per adsorption site is small. These features lead to more complex treatment of polymer adsorption and characterization of the adsorbed layer compared to those of small rigid molecules.

Progress during the past several decades on treatment of adsorbed polymer layers has encompassed both theoretical and experimental aspects. Theoretically, there are two schools of thought, commonly referred to as "scaling" and "mean field", both of which are extensions of polymer solution theories. The most significant of these examples are the theories of de Gennes^{1,2} and of Silberberg³ and Scheutjens and Fleer,^{4,5} respectively. Scaling theories provide global information with emphasis on universality of the properties of adsorbed polymers, while mean field theories provide more detailed descriptions with emphasis on entropic factors. The range of validity of these theories has been discussed elsewhere in the literature.^{6,7}

Experimentally, it has only been in the recent past, with developments in spectroscopic and scattering techniques and the surface force apparatus, that measurements of adsorbed layers have been possible. Convergence of experimental results with theoretical predictions, however, is still in a developing stage. The common setbacks of most experimental techniques are their limited sensitivities to different regions of the concentration profile. For example, ellipsometry and ATR give only the average or effective thickness of an adsorbed layer.⁸ To probe the inner zones which contain loops and tails, dynamic methods such as viscometry⁹ or electrophoretic mobility^{10,11} must be employed. These techniques risk per-

turbing the equilibrium of the adsorbed layer. Surface force measurements have been shown to be a potential method to study the conformation of adsorbed layers.^{12,18} This method measures long-range forces between adsorbed layers and is therefore more sensitive to that portion of the adsorbed layer which is far from the interface. Fluorescence techniques require the incorporation of foreign molecules in the system; it is not evident that local environments around these molecules are not modified. In small-angle neutron scattering, the structures of adsorbed layers have been studied by using the technique of contrast matching.^{19–22}

A relatively recent technique that has proven to be a powerful tool for probing interfacial structures is neutron reflectivity. It is similar to other reflectivity techniques but has several distinct advantages. Due to the fact that neutrons are negligibly absorbed by most materials, the penetration depth of an incident beam of neutrons, depending upon the incident angle, can be of the order of a few centimeters while maintaining a high spatial resolution of a few angstroms. In addition, the neutron scattering length varies randomly from one element to another; the twofold advantages that result are (i) light elements can be studied equally well as heavy ones and (ii) the index of refraction can be modified by isotopic substitution without altering the system chemically. The study of organic compounds has thus benefited fully from these factors. Neutron reflectivity has been used to investigate surfactant^{23,24} and polymeric systems.^{25–29}

In the present study, we have used neutron reflectivity to probe the density profile of a linear, flexible polymer adsorbed from a good solvent at the liquid/air interface. We have also compared our results with surface tension data and to predictions of scaling theory.

Principles of Neutron Reflectivity

Neutron reflectivity is governed by the same principles as those underlying electromagnetic radiation. The reflectivity function can be calculated by starting from the Schrödinger equation for coherent elastic scattering given by³⁰

$$(\hbar^2/2m)\Delta\Psi + E\Psi = V\Psi \quad (1)$$

where Ψ is the neutron wave function, E the incident neutron energy, m the neutron mass, and V the potential

* Author to whom correspondence should be addressed.

that represents the effective interaction of neutron with the medium. At an interface, the wave propagation is²⁸

$$\psi''(z) + k_0^2(n^2(z) - \cos^2 \theta_0)\psi(z) = 0 \quad (2)$$

$k_0 = 2\pi/\lambda$ is the incident wave vector, θ_0 the incident angle, and $n(z)$ the refractive index at distance z from the interface. Neglecting absorption, the neutron refractive index n is defined as³⁰

$$n = 1 - (Nb/2\pi)\lambda^2 \quad (3)$$

where λ is the neutron wavelength, N the number density, and b the average coherent scattering length. From Snell's law, one obtains approximately³⁰

$$\lambda_c = \theta_0(\pi/Nb)^{1/2} \quad (4)$$

where λ_c is the critical wavelength. This relationship permits the use of the *time-of-flight* method,³¹ where the incident angle is fixed and neutrons with a distribution of wavelengths are employed. Total reflection is obtained for $\lambda > \lambda_c$. This method, which avoids changes in incident angles and movement of the sample, facilitates measurements of liquid surfaces.

Reflectivity is defined as the ratio of the intensity of specularly reflected beam to the intensity of incident beam. The reflectivity profile is thus a function of the wave vector transfer, q , perpendicular to the reflecting surface where $q = 4\pi \sin \theta/\lambda$. From eq 4, the critical wave vector transfer is $q_c = 4(\pi Nb)^{1/2}$. For $z > 0$, eq 2 is derived to be³²

$$\Psi''(z) + q_0^2 \Psi(z) = \bar{V}(z)\Psi(z) \quad (5)$$

where $q_0 = q/2$ and $\bar{V}(z) = 4\pi(Nb_p - Nb_s)(\phi(z) - \phi_b)$. Nb_p and Nb_s are scattering length densities of pure monomer and pure solvent molecule, respectively, and $\phi(z)$ and ϕ_b are volume fractions of polymer at distance z from the interface and in the bulk solution, respectively. The reflectivity, R , can be expressed as³²

$$R = \left| \frac{\psi(0) - \frac{1}{iq_0}\psi'(0)}{\psi(0) + \frac{1}{iq_0}\psi'(0)} \right|^2 \quad (6)$$

ψ is the physical solution of eq 5. Detailed derivations and discussions of these equations can be found in ref 32 and 33.

For a homogeneous and structureless interface where the refractive index varies as a step function from one medium to the other (Fresnel), the reflectivity, R_F , is simplified to³⁴

$$R_F(x) = \frac{2x^2 - 1 - 2x(x^2 - 1)^{1/2}}{2x^2 - 1 + 2x(x^2 - 1)^{1/2}} \quad (7)$$

where $x = q/q_c$. For a nonhomogeneous surface, the deviation of the reflectivity from the Fresnel reflectivity provides information on the variations of the refractive index $n(z)$ perpendicular to the interface as a function of the distance, z , from the interface. Since the refractive index is a function of the scattering length density of the atom, one can therefore deduce the composition of the interface.

A method commonly used to calculate a reflectivity function consists of replacing the continuous function $\bar{V}(z)$ by a series of discrete homogeneous layers. The standard optical methods are then applied to determine the Fresnel reflection and transmission coefficients at each interface.^{34,35} In the case of a discrete layer in between two

Table I
Characteristic Properties of PDMS

| polymer | M_w | R_g , Å | M_w/M_n |
|---------|---------|-----------|-----------|
| d-PDMS | 19 000 | 52 | 2.28 |
| d-PDMS | 84 000 | 110 | 1.29 |
| d-PDMS | 800 000 | 510 | 2.00 |
| h-PDMS | 425 000 | 320 | 1.93 |

bulk substrates, the reflectivity is reduced to³⁴

$$R = \frac{r_{12}^2 + r_{23}^2 + 2r_{12}r_{23} \cos(2\beta)}{1 + r_{12}^2 + r_{23}^2 + 2r_{12}r_{23} \cos(2\beta)} \quad (8)$$

r is the Fresnel reflectivity coefficient and

$$r_{ij} = \frac{n_i \sin \theta_i - n_j \sin \theta_j}{n_i \sin \theta_i + n_j \sin \theta_j} \quad \beta = \frac{2\pi}{\lambda} n_2 d_2 \sin \theta_2$$

The subscripts 1 and 3 denote the bulk substrates above and below the interfacial layer 2, respectively, and d_2 is the thickness of the layer. In the presence of surface roughness, the reflectivity function can be modified with an introduction of a Debye-Waller factor.^{36,37}

Another method is an integral form which relates the deviation of the specularly reflected intensity from that of Fresnel's to the square of the Fourier transform of the derivative of the refractive index profile.³⁸

Experimental Section

Surface tension measurements were carried out by using the ring method using a Kruss tensiometer. The value obtained for pure toluene is 28.4 mN m⁻¹, in good agreement with literature value.³⁹

Neutron reflectivity experiments were conducted on the prototype time-of-flight reflectometer DESIR in the ORPHEE reactor. A detailed description of the reflectometer has been given elsewhere.⁴⁰ The neutron wavelengths range from 3 to 15 Å, and the incident angles are $\sim 0.40^\circ$ and $\sim 1.16^\circ$ for the deuterated and protonated polymer systems, respectively. Only three decades of reflectivity are recorded due to the low intensity of the incident beam. The angular resolution of the spectrometer (5–10%) is determined by using high-purity solvents such as deuterated water, toluene, and benzene.

We have studied two systems with different isotopic compositions: deuterated PDMS ($Nb = 5.01\text{E-}6 \text{ Å}^{-2}$) in protonated toluene ($Nb = 0.943\text{E-}6 \text{ Å}^{-2}$) (d-PDMS/h-toluene) and protonated PDMS ($Nb = 0.064\text{E-}6 \text{ Å}^{-2}$) in deuterated toluene ($Nb = 5.72\text{E-}6 \text{ Å}^{-2}$) (h-PDMS/d-toluene). These systems give dissimilar reflectivity results due to different scattering densities of the components, but since isotopic substitution does not alter the system chemically, one can therefore obtain the same information concerning the physical properties. The study of the two complementary isotopic systems thus provides an excellent check of the interpretations of the measurements.

Both the protonated and deuterated polymers are fractionated and characterized by gel permeation chromatography and low-angle light scattering.⁴¹ The molecular weights and radii of gyration are given in Table I. In the present study, reflectivity measurements have been carried out on solutions with bulk concentrations ϕ_b ranging from $\phi^*/10$ to $2\phi^*$, where ϕ^* is the overlap concentration given by

$$\phi^* = 3M_w/4\pi N_A (R_g^2)^{3/2} \quad (9)$$

where R_g is the radius of gyration at infinite dilution.

The sample cells ($100 \times 40 \times 1 \text{ mm}$) are made of either cadmium or aluminum. The former facilitates adjustment of sample position to optimize the detection of reflected beam, while the latter permits simultaneous measurement of the refracted beam. In this paper, we will present only results of specularly reflected beam. During data acquisition, the sample cell is enclosed in a quartz cell to minimize evaporation of the solvent. Data acquisition time is between 5 and 15 h per spectrum.

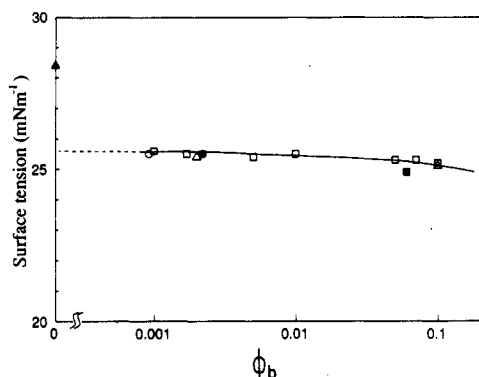


Figure 1. Surface tension as a function of volume fraction of polymer for pure solvent (Δ); h-PDMS, $M_w = 116\,500$ (\square); h-PDMS, $M_w = 510\,000$ (Δ); h-PDMS, $M_w = 4\,200\,000$ (\circ); d-PDMS, $M_w = 800\,000$ (\bullet); d-PDMS, $M_w = 84\,000$ (\blacksquare).

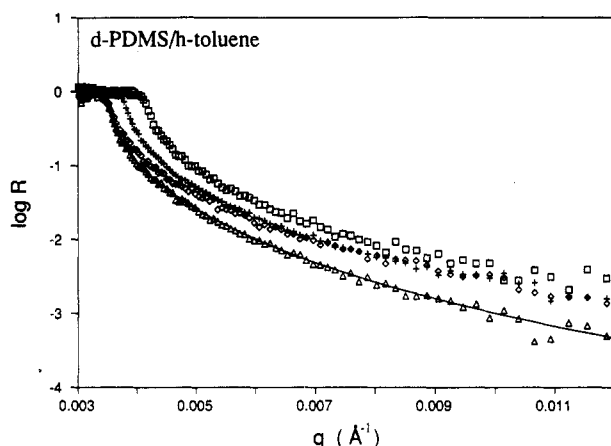


Figure 2. Log reflectivity versus q of d-PDMS/h-toluene systems at $2\phi^*$ for pure toluene (Δ), $M_w = 800\,000$ (\diamond), $M_w = 84\,000$ ($+$), and $M_w = 19\,000$ (\square). The solid line is the calculated Fresnel curve for pure toluene.

Results and Discussion

Figure 1 shows the surface tension results of d-PDMS and h-PDMS in toluene as a function of volume fraction of polymer ϕ_b for samples of different molecular weights. These results are in agreement with those obtained by Ober et al.³⁹ As expected, the interfacial tension does not depend on the molecular dimension nor on the isotopic composition of the polymer. The latter justifies our assumption that the reflectivity results of different isotopic systems should furnish the same information on the physical properties of the system.

Figure 2 shows reflectivity curves of pure h-toluene and of d-PDMS/h-toluene solutions as a function of wave vector transfer q . The deviations of the polymer solution reflectivity curves from that of pure solvent in the high q regions are due to the presence of interfacial structure arising from the adsorbed polymers. Near the critical reflection edge, however, deviations are solely attributed to the difference in refractive indices of the bulk solutions. This is clearly seen in the increase in displacement of the critical reflection edge with increase in volume fraction of polymer present in the solution as the molecular weight decreases (at fixed concentration, $2\phi^*$). The results reported before²⁸ might have been due to this bulk effect.

For pure toluene, the experimental results can be seen to agree very well with a calculated Fresnel curve (solid line; $Nb = 0.943E-6 \text{ \AA}^{-2}$). Thus, we do not detect a sensitivity of the reflectivity curve toward surface roughness induced by thermal fluctuations of the toluene surface. The surface roughness arising from these fluctuations

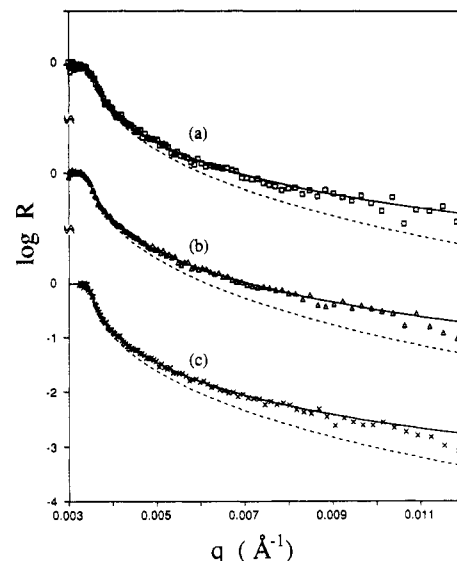


Figure 3. Comparisons of calculated reflectivities using the two-layer step profile (solid lines) with experimental data for d-PDMS/h-toluene systems ($\phi_b = \phi^*/10$) for $M_w = 19\,000$ (a) (\square), $M_w = 84\,000$ (b) (Δ), and $M_w = 800\,000$ (c) ($+$). The dashed lines are corresponding Fresnel curves.

depends on the surface tension of the liquid, which is estimated to be about 5 \AA for toluene. It is noted that the effect of surface roughness on reflectivity is dependent upon the neutron wavelengths used and can be a significant factor for reflectivity values less than 10^{-4} .^{42,43}

Two-Layer Step Profile. For polymer solutions, the presence of interfacial structure due to adsorbed polymers produces a significant deviation of reflectivity from the Fresnel case. This deviation is positive for the case of d-PDMS/h-toluene and negative for that of h-PDMS/d-toluene. Curves a–c of Figure 3 show the reflectivity data together with the corresponding calculated Fresnel curves (in dashed lines) for the deuterated polymer samples of molecular weights 19 000, 84 000, and 800 000, respectively, at bulk concentration $\phi^*/10$. The continuous lines through the experimental data are reflectivity curves calculated (by the optical matrix method) by using a two-layer model. The first layer, L_1 , has a scattering density of $5.01E-6 \text{ \AA}^{-2}$, corresponding to that of pure deuterated polymer. The thickness of this layer is between 10 and 15 \AA , about 2–3 times the monomer size, and is independent of polymer molecular weight and bulk concentration provided there is sufficient polymer to fill the surface. The second layer, L_2 , has a scattering density ranging from 2 to 10 times that of the bulk depending upon the bulk concentration. L_2 is of the order of the radius of gyration of the polymer.

Qualitatively, the fact that a simple two-layer model can be used to describe the experimental data is rather surprising; introduction of a third layer does not produce any detectable improvement on the fit of the data. Quantitatively, however, the amount of polymer adsorbed at the surface estimated from this model is not consistent with that evaluated from surface tension data. Thus, in spite of an apparent success to describe the data, the model is clearly oversimplified. It has, however, permitted us to identify two cut-off regions, the physical importance of which is described below. From the above analysis, the importance of using other techniques to complement reflectivity studies therefore cannot be overlooked.

Self-Similar Profile. With a knowledge of the cut-off points in the concentration profile, we then analyzed the data with a more realistic model such as that predicted by scaling theory,¹ where the density profile of the adsorbed

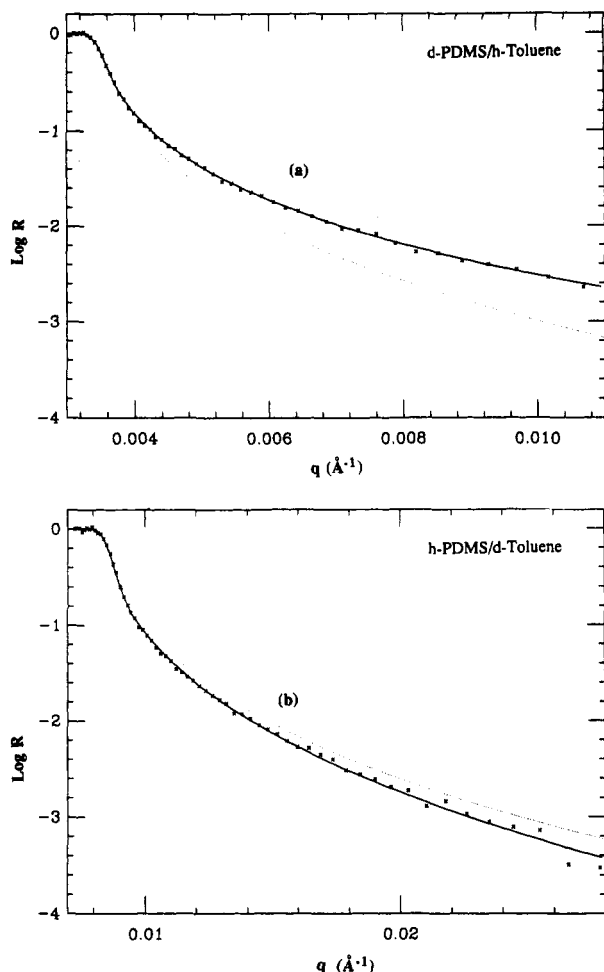


Figure 4. Comparisons of calculated reflectivities using the *self-similar profile* (solid lines) with experimental data for d-PDMS/h-toluene (a) and h-PDMS/d-toluene (b) systems ($\phi_b = \phi^*/10$). The dotted lines correspond to Fresnel curves.

polymer layer is expected to exhibit a smooth decay toward the bulk. Such a profile cannot be calculated conveniently by using the optical matrix method. The reflectivity functions in this section are thus calculated by using a continuous function $\bar{V}(z)$ described in eq 5.

Curves a and b of Figure 4 show the reflectivity data ($\phi_b = \phi^*/10$) of d-PDMS/h-toluene and h-PDMS/d-toluene, respectively, together with their corresponding Fresnel curves (dotted lines). The continuous lines passing through the experimental points in these figures are reflectivity curves calculated by using a concentration profile of self-similar structure described by de Gennes.¹ This model consists of a region in close proximity to the surface, the monomer-rich zone, D , referred to as the *proximal zone* by de Gennes.¹ D in our case is determined to be 10–15 Å and is *independent of molecular weight and bulk concentration* provided there is sufficient polymer to form a saturated layer. This zone is similar to L_1 described in the two-layer model above except that the surface concentration ϕ_s in this case is 0.4. Within this proximal zone, surface potential and short-range interactions of monomers and the surface are felt. This region also determines the overall amount of polymer adsorbed and the interfacial tension of the adsorbed layer in equilibrium with an infinitely dilute solution. A detailed discussion of the significance and universality of this zone has been given by des Cloizeaux.⁴⁴

The values of D and ϕ_s can now be shown to be consistent with surface tension results from the relationship⁴⁵ $a^2\gamma_1/kT = \delta$, where a is the monomer size, γ_1 the interaction

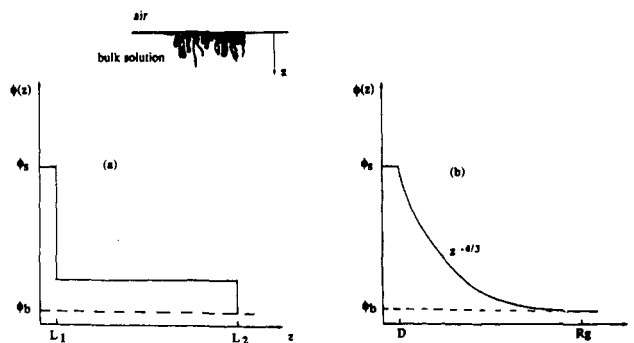


Figure 5. Schematic representations of the two-layer step profile (a) and the self-similar profile (b).

energy of monomer with the surface, and δ the fraction of monomer in the surface region. $\gamma_1\delta$ is the surface tension between pure solvent and an adsorbed layer of polymer in equilibrium with an infinitely dilute solution. From surface tension and reflectivity data, respectively, $\gamma_1\delta = 2.8 \text{ mN m}^{-1}$ and $\delta = \phi_s = 0.4$; one thus obtains $\gamma_1 = 6.9 \text{ mN m}^{-1}$. Taking the monomer size $a = 5 \text{ Å}$ and $D = 12.5$ (from reflectivity data), we get $a^2\gamma_1/kT = \delta = a/D = 0.4$. Thus, the model that we have used to describe the reflectivity data is consistent with surface tension measurements. These results also show that $a < D$ and $a^2\gamma_1/kT < 1$, conforming to a strong adsorption and weak coupling limit, which has been shown to be the case for PDMS/toluene system.³⁹

Beyond D , the concentration profile decreases with a self-similar structure predicted by de Gennes¹ up to a second cut-off ξ_b , the bulk characteristic length. The limiting value of ξ_b is R_g , the radius of gyration in the case of dilute solution. In this case, the cut-off depends, naturally, on the molecular weight of the polymer. From the concentration dependence of the characteristic length, $\xi_b \sim \phi_b^{-3/4}$, the monomer density in this region scales as $\phi(z) \sim (a/z)^{4/3}$, where $\phi(z)$ is the volume fraction of monomer and z the distance from the interface.¹ In this *central zone* ($D < z < R_g$) which consists of loops and tails, only repulsive forces between monomers exist, and it is this repulsion that creates a self-similar structure in the adsorbed layer. Except for the cut-off mentioned above, the experimental results show that this profile is universal and independent of molecular weight and bulk concentration (for $\phi_b < \phi^*$). The self-similar nature of the adsorbed polymer layer that we have observed here is in agreement not only with theoretical predictions but also with results obtained from neutron scattering experiments on PDMS adsorbed from cyclohexane onto silica surface.²² Thus, the concentration profile for this polymer adsorbed physically is independent of the nature of the interface. We are currently testing other profiles such as the exponential profile and the power law profile using values other than $4/3$ as the exponent.

At larger distances from the interface ($z > \xi_b$), the profile is predicted to decrease exponentially toward the bulk concentration ϕ_b .¹ Our reflectivity measurements, however, are not sufficiently sensitive to the relaxation in this zone due to the very small differential monomer concentration in this zone and that of the bulk solution. A schematic representation of the two-layer profile and the self-similar profile is shown in Figure 5.

Conclusions

We have used neutron reflectivity to characterize the concentration profile of a linear flexible polymer adsorbed from a good solvent at the liquid/air interface. The profile is found to exhibit a self-similar structure as predicted by

scaling theory. The characteristic parameters obtained, D and a , conform to surface tension results which support a strong adsorption and weak coupling case for the system studied. In addition, both D and the concentration profile are found to be independent of polymer molecular weight and bulk concentration. This universality is in agreement with predictions of scaling theory.

Acknowledgment. We appreciate discussions with Dr. G. Jannink, who has been a constant source of motivation and encouragement in this work.

References and Notes

- (1) de Gennes, P. G. *Macromolecules* **1981**, *14*, 1637.
- (2) de Gennes, P. G. *Macromolecules* **1980**, *13*, 1069.
- (3) Silberberg, A. *J. Chem. Phys.* **1968**, *48*, 2835.
- (4) Scheutjens, J. M. H. M.; Fleer, G. J. *J. Phys. Chem.* **1979**, *83*, 1619.
- (5) Scheutjens, J. M. H. M.; Fleer, G. J. *J. Phys. Chem.* **1980**, *84*, 178.
- (6) Schaefer, D. W. *Polymer* **1984**, *25*, 387.
- (7) Fleer, G. J.; Scheutjens, J. M. H. M.; Cohen Stuart, M. A. *Colloids Surf.* **1988**, *31*, 1.
- (8) Lipatov, Y. S.; Sergeeva, L. M. *Adsorption of Polymers*; Wiley: New York, 1974.
- (9) Pefferkorn, E.; Dejardin, P.; Varoqui, R. *J. Colloid Interface Sci.* **1978**, *63*, 353.
- (10) Koopal, L. K.; Lyklema, J. *Faraday Discuss. Chem. Soc.* **1975**, *59*, 230.
- (11) Brooks, D. E. *J. Colloid Interface Sci.* **1973**, *43*, 687.
- (12) Israelachvili, J. N.; Tirrell, M.; Kelen, J.; Almog, Y. *Macromolecules* **1984**, *17*, 204.
- (13) Hadziioannou, G.; Patel, S.; Granick, S.; Tirrell, M. *J. Am. Chem. Soc.* **1986**, *108*, 2869.
- (14) Tirrell, M.; Patel, S.; Hadziioannou, G. *Proc. Natl. Acad. Sci. U.S.A.* **1987**, *84*, 4725.
- (15) Patel, S.; Tirrell, M.; Hadziioannou, G. *Colloids Surf.* **1988**, *31*, 157.
- (16) Ansarifard, M. A.; Luckham, P. F. *Polymer* **1988**, *29*, 329.
- (17) Taunton, H. J.; Toprakcioglu, C.; Klein, J. *Macromolecules* **1988**, *21*, 3333.
- (18) Marra, J.; Hair, M. L. *Colloids Surf.* **1988**, *34*, 215.
- (19) Barnett, K. G.; Cosgrove, T.; Vincent, B.; Burgess, A. W.; Crowley, T. L.; King, T.; Turner, J. D.; Tadros, Th. F. *Polym. Commun.* **1981**, *22*, 283.
- (20) Barnett, K. G.; Cosgrove, T.; Crowley, T. L.; Tadros, Th. F.; Vincent, B. In *The Effect of Polymer in Dispersion Properties*; Tadros, Th. F., Ed.; Academic Press: London, 1982; p 183.
- (21) Cosgrove, T.; Crowley, T. L.; Vincent, B.; Barnett, K. G.; Tadros, Th. F. *Faraday Symp. Chem. Soc.* **1982**, *16*, 101.
- (22) Auvray, L.; Cotton, J. P. *Macromolecules* **1987**, *20*, 202.
- (23) Bradley, J. E.; Lee, E. M.; Thomas, R. K.; Willatt, A. J.; Penfold, J.; Ward, R. C.; Gregory, D. P.; Waschkowski, W. *Langmuir* **1988**, *4*, 821.
- (24) Lee, E. M.; Thomas, R. K.; Penfold, J.; Ward, R. C. *J. Phys. Chem.* **1989**, *93*, 381.
- (25) Fernandez, M. L.; Higgins, J. S.; Penfold, J.; Ward, R. C.; Shackleton, C.; Walsh, D. J. *Polymer* **1988**, *29*, 1923.
- (26) Russell, T. P.; Karim, A.; Mansour, A.; Felcher, G. P. *Macromolecules* **1988**, *21*, 1890.
- (27) Anastasiadis, S. H.; Russell, T. P.; Satija, S. K.; Majkrzak, C. F. *Phys. Rev. Lett.* **1989**, *62*, 1852.
- (28) Sun, X.; Bouchaud, E.; Lapp, A.; Farnoux, B.; Daoud, M.; Jannink, G. *Europhys. Lett.* **1988**, *6*, 207.
- (29) Rennie, A. R.; Crawford, R. J.; Lee, E. M.; Thomas, R. K.; Crowley, T. L.; Roberts, S.; Qureshi, M. S.; Richards, R. W. *Molecules* **1989**, *22*, 3466.
- (30) Werner, S. A.; Klein, A. G. In *Neutron Scattering*; Skold, K., Price, D. L., Eds.; Academic Press: New York, 1986.
- (31) Farnoux, B. *Proceedings, Neutron Scattering in the Nineties*; IAEA: Vienna, 1985.
- (32) Guiselin, O. *J. Phys. (Paris)* **1989**, *50*, 3407.
- (33) Dietrich, S.; Schack, R. *Phys. Rev. Lett.* **1987**, *58*, 140.
- (34) Born, M.; Wolf, E. *Principles of Optics*; Pergamon Press: Oxford, U.K., 1975.
- (35) Lekner, J. *Theory of Reflection*; Martinus Nijhoff: Dordrecht, The Netherlands, 1987.
- (36) Beckman, P.; Spizzichino, A. *The Scattering of Electromagnetic Waves from Rough Surfaces*; Pergamon Press: New York, 1963.
- (37) Nevot, L.; Croce, P. *Rev. Phys. Appl.* **1980**, *15*, 761.
- (38) Als-Nielsen, J. *Z. Phys. B* **1985**, *61*, 411.
- (39) Ober, R.; Paz, L.; Taupin, C.; Pincus, P.; Boileau, S. *Macromolecules* **1983**, *16*, 50.
- (40) Farnoux, B. *Rapport d'Activité*; Laboratoire Léon Brillouin, CEA, Gif-sur-Yvette, France, 1987-1988.
- (41) Lapp, A.; Herz, J.; Strazielle, C. *Makromol. Chem.* **1985**, *186*, 1919.
- (42) Braslau, A.; Deutsch, M.; Pershan, P. S.; Weiss, A. H.; Als-Nielsen, J.; Bohr, J. *Phys. Rev. Lett.* **1985**, *54*, 114.
- (43) Garoff, S.; Sirota, E. B.; Sinha, S. K.; Stanley, H. B. *J. Chem. Phys.* **1989**, *90*, 7505.
- (44) des Cloizeaux, J. *J. Phys. (Paris)* **1988**, *49*, 699.
- (45) de Gennes, P. G.; Pincus, P. *J. Phys. Lett.* **1983**, *44*, L241.